

Longitudinal transcriptional analysis of developing neointimal vascular occlusion and pulmonary hypertension in rats

Laszlo T. Vaszar,¹ Toshihiko Nishimura,¹ John D. Storey,² Guohua Zhao,¹
Daoming Qiu,¹ John L. Faul,¹ Ronald G. Pearl,³ and Peter N. Kao¹

¹Division of Pulmonary/Critical Care Medicine, ³Department of Anesthesiology, Stanford University Medical Center, Stanford, California 94305-5236; and ²Department of Biostatistics, University of Washington, Seattle, Washington 98195-7232

Submitted 1 December 2003; accepted in final form 16 January 2004

Vaszar, Laszlo T., Toshihiko Nishimura, John D. Storey, Guohua Zhao, Daoming Qiu, John L. Faul, Ronald G. Pearl, and Peter N. Kao. Longitudinal transcriptional analysis of developing neointimal vascular occlusion and pulmonary hypertension in rats. *Physiol Genomics* 17: 150–156, 2004; 10.1152/physiolgenomics.00198.2003.—Pneumonectomized rats injected with the alkaloid toxin, monocrotaline, develop progressive neointimal pulmonary vascular obliteration and pulmonary hypertension resulting in right ventricular failure and death. The antiproliferative immunosuppressant, triptolide, attenuates neointimal formation and pulmonary hypertension in this disease model (Faul JL, Nishimura T, Berry GJ, Benson GV, Pearl RG, and Kao PN. *Am J Respir Crit Care Med* 162: 2252–2258, 2000). Pneumonectomized rats, injected with monocrotaline on day 7, were killed at days 14, 21, 28, and 35 for measurements of physiology and gene expression patterns. These data were compared with pneumonectomized, monocrotaline-injected animals that received triptolide from day 5 to day 35. The hypothesis was tested that a group of functionally related genes would be significantly coexpressed during the development of disease and downregulated in response to treatment. Transcriptional analysis using total lung RNA was performed on replicate animals for each experimental time point with exploratory data analysis followed by statistical significance analysis. Marked, statistically significant increases in proteases (particularly derived from mast cells) were noted that parallel the development of vascular obliteration and pulmonary hypertension. Mast-cell-derived proteases may play a role in regulating the development of neointimal pulmonary vascular occlusion and pulmonary hypertension in response to injury.

proteinases; gene expression analysis; mast cells; monocrotaline

PULMONARY VASCULAR OBLITERATION is the central pathophysiological process of primary pulmonary hypertension (PPH), leading ultimately to fatal right ventricle failure (23). The pathophysiology of pulmonary hypertension involves neointimal and medial proliferation and hypertrophy of vascular smooth muscle cells (SMCs) and endothelial cells (ECs), and adventitial fibrosis (8). The quest for a rodent model of pulmonary hypertension with neointimal vascular occlusion led to the pneumonectomy-monocrotaline model (20), in which increased shear stress and compensatory lung hypertrophy (induced by the pneumonectomy) modifies the monocrotaline response in small intra-acinar pulmonary arteries, converting it to a neointimal response (28). In this model, rats demonstrate an initial gradual increase in pulmonary arterial and right

ventricular systolic pressures (RVSPs), which accelerate markedly after day 21 until death around day 40 (7). Using this model, we demonstrated that simvastatin attenuates disease progression (17) and rescues rats from fatal pulmonary hypertension by inducing apoptosis of neointimal SMCs(18).

We report here the results of a longitudinal array-based parallel mRNA expression pattern analysis during the development of the vascular obliteration and pulmonary hypertension in the pneumonectomy-monocrotaline model of hypertensive pulmonary vascular disease in rats. Our focus was to interrogate gene expression analysis in parallel with histopathological (vascular occlusion scores) and physiological (RVSPs) measurements. We hypothesized that a group of functionally related genes would be consistently and statistically significantly coexpressed during the development of disease and downregulated in response to treatment.

We also compared global gene expression in animals administered triptolide and in untreated animals (receiving vehicle). Triptolide is a diterpenoid triepoxide purified from *Tripterygium wilfordii hook f*, with immunosuppressive, anti-inflammatory and antiproliferative properties (32). Our group has shown that triptolide treatment in a preventive schedule attenuates the development of pulmonary hypertension in this model (7). Compared with the rats that received vehicle alone, rats treated with triptolide between days 5 and 35 had diminished RVSP, pulmonary arterial pressure, and right ventricular mass (7). Histology revealed severe changes of pulmonary vascular obliteration in the vehicle-treated rats but not in the triptolide-treated rats (7). Here, we present data suggesting that the global gene expression pattern also resembles that seen in intermediate stages of severity.

To our knowledge, this is the first reported array-based longitudinal time course analysis of pulmonary vascular remodeling in a complex mammalian system using replicates and statistical significance analysis.

METHODS

Animal model. Pneumonectomy (day 0) followed at day 7 by one injection of monocrotaline (60 mg/kg intraperitoneally) was performed on 12-wk-old male Sprague-Dawley rats (weight 350–400 g) as described (7). The left lung is immediately frozen in liquid nitrogen and stored at -80°C . These lungs serve as sources for control (normal) lung RNA. RVSPs were measured prior to death on three rats at each time point, days 0, 14, 21, 28, 35 (0, V14, V21, V28, V35) and triptolide treated at day 35 (T35), as described (7). All animals received humane care; the study was approved by the Stanford Panel on Laboratory Animal Care.

Array experiments. Lungs from the euthanized animals were homogenized, and total RNA was extracted. To increase the statistical

Article published online before print. See web site for date of publication (<http://physiolgenomics.physiology.org>).

Address for reprint requests and other correspondence: P. N. Kao, Pulmonary/Critical Care Medicine, Stanford Univ. Medical Center, Stanford, CA 94305-5236 (E-mail: peterkao@stanford.edu).

power, six normal lungs were used (*day 0*). One lung from *V14* was lost in storage, so two rats at *V14* were analyzed. The remaining time points (*V21*, *V28*, *V35*, *T35*) had three animals each. Radiolabeled cDNA probes generated from 50 μg of tRNA were Southern hybridized to nylon arrays containing 1,176 genes (Atlas Rat 1.2 Array, model 7854-1; Clontech). Signals were quantified using a Cyclone PhosphorImager and OptiQuant software (Packard Instruments). The raw expression levels were log transformed, then median centered within each array using Microsoft Excel. The microarray data comply with the MIAME standard and are available for review at the Gene Expression Omnibus (GEO) database at the National Center for Biotechnology Information (<http://www.ncbi.nlm.nih.gov/geo/>). The accession number for this data series is GSE843.

Data analysis. For exploratory data analysis, the expression replicates were averaged for each time point. The k-means analysis and average-linkage hierarchical clustering of the averages for each time point was performed using J-Express software (6). To detect statistically significant differentially expressed genes, we used all the array replicates and employed the "significance analysis of microarray" (SAM) software (25, 29) to perform a modified ANOVA test on the genes. This procedure measures the statistical significance of the relationship between gene expression and the multiclass grouping in terms of the false discovery rate (26).

Northern blot. Fifteen micrograms of total lung RNA was fractionated on a 1% agarose, 2.2 M formaldehyde gel, and transferred overnight to a nylon membrane by capillary transfer. The membrane was UV irradiated, then prehybridized for 30 min at 65°C in hybridization solution (QuikHyb, Stratagene), and hybridized with the addition of radiolabeled probe and salmon sperm DNA at 60°C for 2 h. Blots were washed at increasing stringency of salt concentration and temperature, with a final wash being in 0.2 \times SSC, 0.1% SDS at 60°C for 20 min. The membranes were exposed to Kodak X-OMAT film at -80°C 12 h for glyceraldehyde-3-phosphate dehydrogenase (GAPDH) and for 24 h for rat mast cell protease-1.

RESULTS

We used transcriptional profiling to identify genes that are differentially expressed and parallel the development and prevention of experimental pulmonary hypertension. Each individual animal was analyzed on a separate array. For the exploratory data analysis, the replicates for a time point were averaged, whereas for statistical significance analysis the replicates were analyzed individually.

Hemodynamics. RVSP increased markedly between *days 21* and *35* (Fig. 1). The peak RVSP of 47 ± 6 mmHg was attained on *day 35*. Triptolide attenuated the increase of RVSP at *day 35* to 29 ± 5 mmHg (7).

Exploratory gene expression analysis using k-means clustering. The gene expression profiles of all the 1,176 genes arrayed in the membrane ranged between a minimum of 0.43 and a maximum of 600.05 (1,494-fold difference). The results of the k-means analysis with 20 clusters are shown in Fig. 2.

Two clusters (ID = 14 and ID = 2 with 8 and 15 genes, respectively) have a longitudinal expression pattern similar to the curve of RVSP. This curve is characterized by a progressive increase in expression during the sampled period, with a peak at *day 35*, and with an attenuated elevation in response to triptolide treatment. *Cluster 14* (Fig. 3, top) consists of the following genes, in decreasing order of expression at *V35*: mast cell protease-1, mast cell chymase-1, adipocyte lipid-binding protein FABP4, macrophage inflammatory protein 1 α , Plasminogen activator inhibitor-1, gelatinase A (matrix metalloproteinase-2), cathepsin D, and cathepsin K. The gene with peak expression at *V35*, mast cell protease-1, has a 21-fold increase

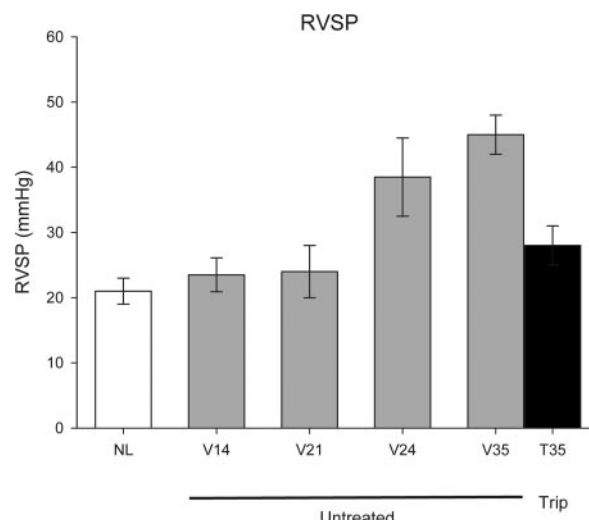


Fig. 1. Right ventricular systolic pressure (RVSP). Pulmonary arterial pressures were measured at baseline (open bar), during the development of experimental hypertensive pulmonary vascular disease (gray bars), and in response to triptolide treatment (black bar). The x-axis represents the experimental time points in days.

in expression between *days 0* (expression value 1.04) and *day 35* (expression value 22.02).

Cluster 2 consists of the following genes (Fig. 3, bottom), in decreasing order of the difference between expressions at *V35* and normal: mast cell protease-7, aldolase B, fructose-biphosphate, cathepsin B, interleukin 18 (IL-18), macrophage inflammatory protein-2, carboxypeptidase E, liver arginase-1, multi-drug resistance protein-1 (P-glycoprotein), cathepsin S, solute carrier family 1, member 3, myristoylated alanine-rich protein kinase C substrate, proteasome 26S subunit 2, acetyl-CoA acyltransferase, proteasome 26S subunit 1, and ras-related protein RAB26. Mast cell protease-7 has registered a 4.7-fold increase in expression between *days 0* (expression value 0.93) and *35* (expression value 4.4).

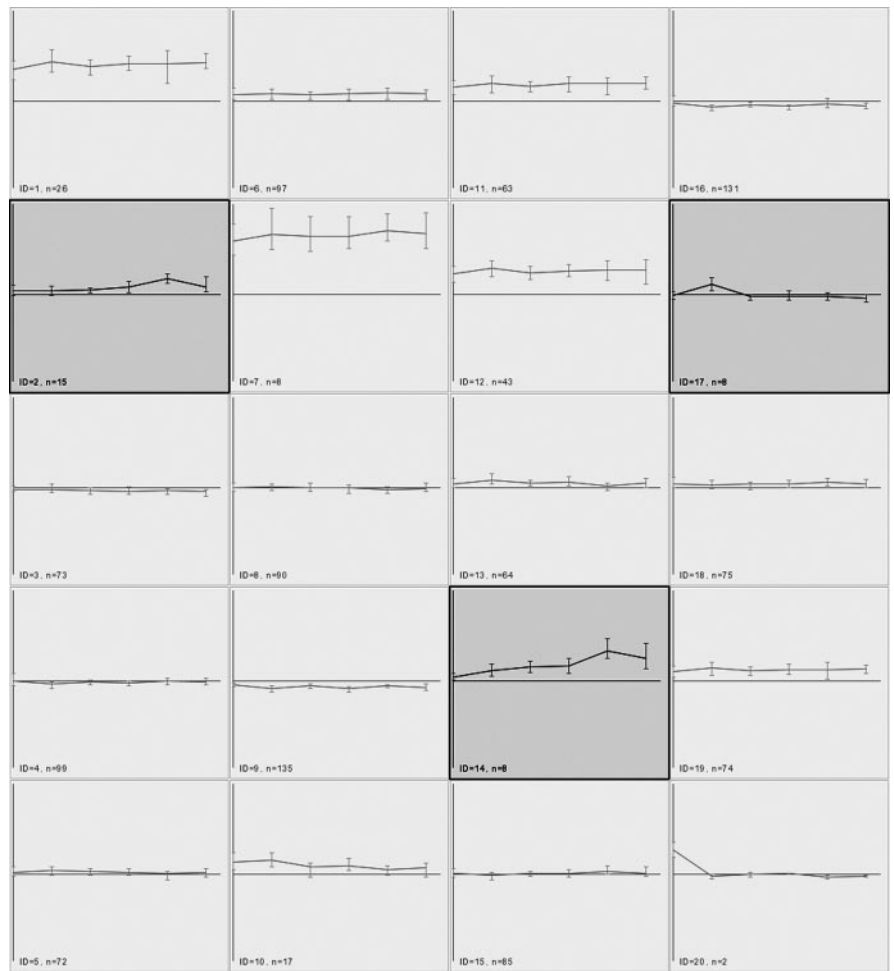
Twelve of the 23 (52%) genes in the two clusters (6 of 8 in *cluster 14* and 6 of 14 in *cluster 2*) are proteases.

Another cluster (ID = 17) of eight genes was noted to peak early (*V14*), followed by return of expression values near baseline (Fig. 4). This cluster included six genes coding for cellular receptors: epidermal growth factor receptor, erbB4 proto-oncogene (HER4), serotonin receptor-5B, and ephrin type A receptors 3, 5, and 7. The genes for calcium channel α A and C-type natriuretic peptide (CNP) completed this cluster.

Statistical significance testing using SAM. Statistical significance of differential expression was assessed using all 20 individual arrays. The 16 most significant genes are shown in Table 1 (top). To illustrate the trend in statistical significance, the next two genes are also included. A *q* value is listed with each gene, which estimates the false discovery rate (proportion of false positives) when using that cutoff for significance (25, 26). The 16 most significant genes all have *q* values of 6.25%, which means that we expect 6.25% (~1 gene among the 16) to be false positives. There is no "safe" value for a *q* value cutoff, and Table 1 (bottom) lists the false discovery rates from among 1 to 25 genes being called significant.

Confirmation of gene expression findings. Beyond confirmation of statistical significance of the aggregate of 16 genes

Fig. 2. Clustering of gene expression data. Each panel represents one cluster from the k-means analysis, which partitions the data set of 1,176 genes into an operator-predetermined number of clusters, by maximizing between-clusters differences relative to within-cluster differences. The optimal number of clusters in this experiment is around 20 (too few clusters yield expression patterns resembling the average for the whole data set, whereas too many will fragment the data, yielding many similar clusters). The x-axis represents the 6 experimental time points: 0, V14, V21, V28, V35, and T35. The y-axis is logarithmic and represents the mean and the range (amplitude) of gene expression. An expression level of zero corresponds to the median value for that time point. All the clusters are represented at the same scale on the y-axis. Two clusters (ID 2 and 14) reveal a longitudinal expression pattern that parallels the evolution of RVSP in Fig. 1, whereas one cluster (ID = 17) reveals an early (*day 14*) peak of expression followed by return to baseline.



called, confirmation of the expression level of mast cell protease was performed with Northern hybridization (Fig. 5).

Hierarchical clustering of experimental time points. Clustering of the data points was performed to investigate the global expression patterns that characterize each experimental time point. The dendrogram (Fig. 6) reveals that the global expression level at *day 35* is an outlier. The global expression of triptolide-treated animals at *day 35* (T35) is between those of *days 21* and *28*, being more similar to the former. The expression level at *day 14* is intermediate between the expression of normal lungs and the composite of early disease (*days 21* and *28*) and treated animals (T35).

DISCUSSION

We used a formal succession of exploratory data analysis, statistical significance testing, and biologic confirmation, to identify genes associated with the development of experimental pulmonary hypertension. In the exploratory phase, we used k-means analysis to identify clusters of genes with a similar pattern of expression (Fig. 2). Clustering is simply a visualization tool that helps the operator identify patterns, but does not provide information of the statistical strength of the identified behavior. Classic statistical hypothesis testing has to be adapted for use in microarray analysis, and we used the SAM, a methodology developed specifically for finding genes with

significantly different expression values in a set of array experiments (25, 29).

Patterns of gene expression. To identify genes potentially involved in the regulation of repair-after-vascular injury, we aimed at identifying genes that mimic the evolution of luminal obliteration (structural behavior) and hemodynamics (physiology behavior, RVSP, Fig. 1) (7). The pattern that emerges from these observations is a relentless increase during the development of obliterative pulmonary vasculopathy compared with normal, peaking at *day 35*, with attenuated disease at *day 35* in triptolide-treated animals (T35). Another pattern (suggestive of acute injury) shows an acute increase from normal to *day 14*, followed by restoration of expression to baseline. The mirror images (e.g., high expression at baseline, progressive decline during the development of the disease, and triptolide-induced increase) of these patterns were also included in the analysis.

Genes with relentless increase in expression. Clusters 14 and 2 reveal a gradual increase from normal throughout the development of the disease. An attenuated expression is noted at *day 35* in triptolide-treated animals compared with vehicle-treated animals. The difference between these two clusters is mainly in the magnitude of the expression values, rather than the shape of the expression graph. Twelve of 22 genes in the two clusters are proteases, with mast-cell-derived proteases featured prominently in these clusters. Significance analysis

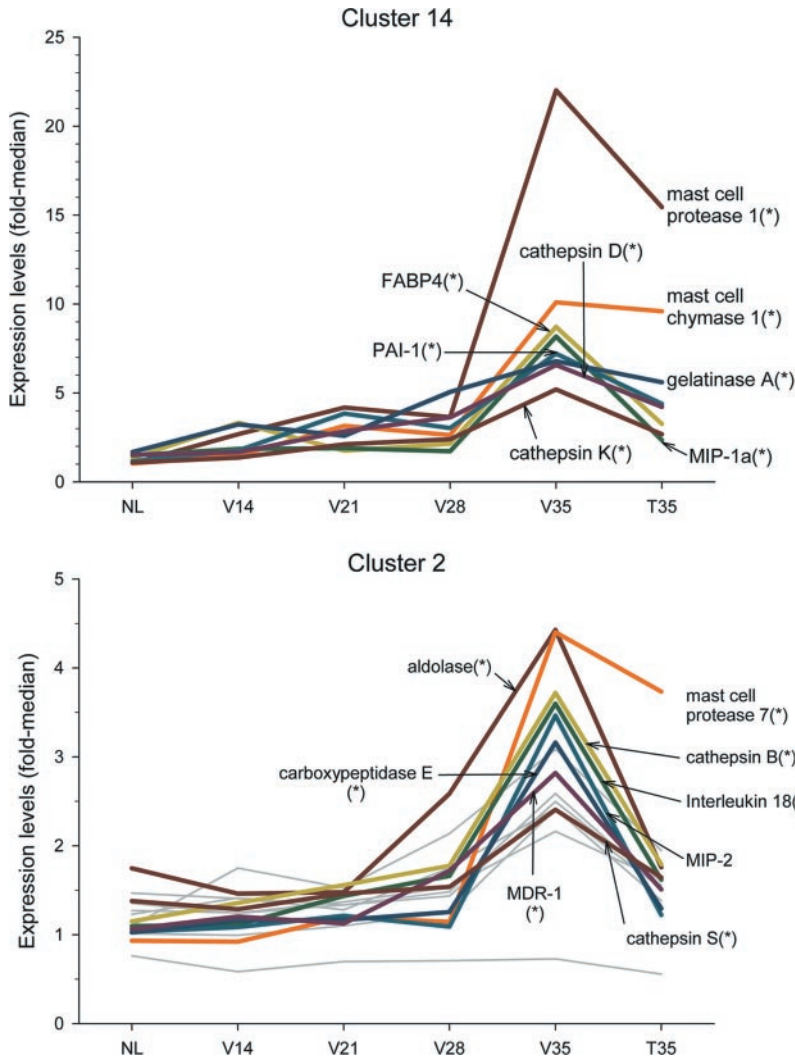


Fig. 3. Longitudinal (time course) expression of genes from clusters 14 (top) and 2 (bottom). These clusters parallel the evolution of hemodynamics during the development of experimental pulmonary hypertension and in response to therapy. The values are median-centered averages of the replicate animals for each of the six experimental time points. *Statistical significance by significance analysis of microarray (SAM) (see text). The faint gray lines in cluster 2 represent genes not labeled in this graph. The complete list of genes in this cluster can be found in the RESULTS. PAI-1, plasminogen activator inhibitor-1; FABP4, adipocyte fatty acid binding protein 4; MIP-1a, macrophage inflammatory protein-1 α ; MDR1, multi-drug resistance protein; MIP-2, macrophage inflammatory protein-2; aldolase, aldolase B, fructose-biphosphate.

Fig. 4. Longitudinal (time course) expression of genes from cluster 17. The genes in this cluster reveal an “acute-phase” response, in that their expression increases after the two-step (pneumonectomy-monocrotaline) injury, and the expression returns to baseline afterwards. EGF, epidermal growth factor.

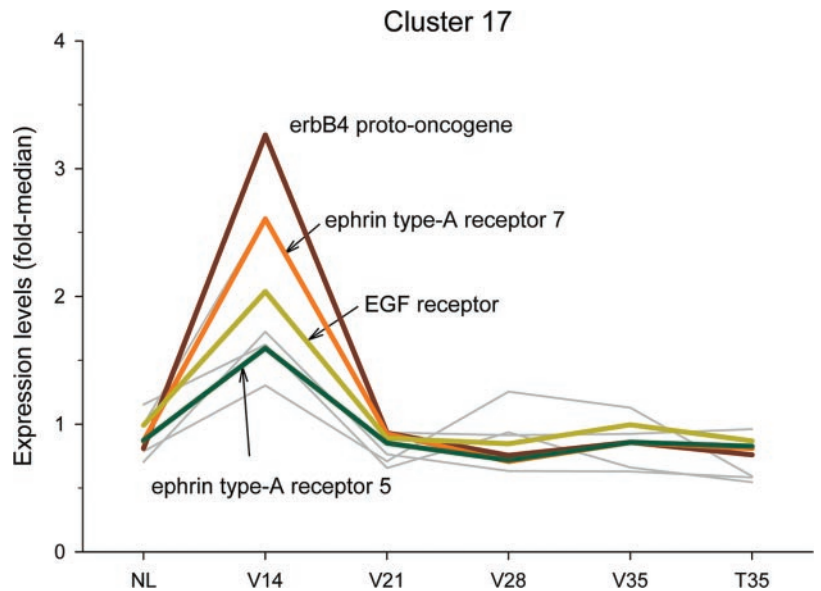


Table 1. Analysis of significance

Significant Genes List (16 genes called)		
Gene Name	Score, d	q Value, %
Mast cell protease-7	0.66	6.25
Mast cell protease-1	0.61	6.25
Interleukin 18	0.58	6.25
Mast cell chymase-1	0.56	6.25
PAI-1 (plasminogen activator inhibitor-1)	0.52	6.25
Vasopressive intestinal peptide receptor	0.50	6.25
Cathepsin D	0.49	6.25
Cathepsin K	0.46	6.25
FABP4 (adipocyte fatty acid-binding protein)	0.46	6.25
MDR-1 (multidrug resistance protein-1)	0.45	6.25
Carboxypeptidase E (CPE); CPH	0.43	6.25
FABP5 (epidermal fatty acid-binding protein)	0.43	6.25
Mast cell protease-6	0.40	6.25
Cathepsin B	0.39	6.25
Aldolase B, fructose-biphosphate	0.38	6.25
MIP-1a (macrophage inflammatory protein 1 α)	0.38	6.25
Cathepsin S	0.38	11.11
Cell-division control protein 25 B	0.36	11.11

Significance		
No. of genes called	Median number of genes falsely called	Median FDR, %
25	7	28.0
21	4	19.0
18	2	11.1
16	1	6.25
12	1	8.3
10	1	10.0
9	1	11.1
7	1	14.3
5	1	20.0
4	1	25.0
2	1	50.0
1	1	100.0

Listing of the 16 genes called "significant" (*top*), based on the relationship between the number of genes called "significant," the number of genes falsely called in the process, and the false discovery rate (FDR, *bottom*). To illustrate the trend in statistical significance, the next two genes are also included. The significance analysis of microarray (SAM) software estimates the false discovery rate (the expected proportion of false positives among the total number of significant genes) for each significance threshold. The *q* value for a gene gives the minimum false discovery rate that can be attained when calling that gene significant and therefore may be equal among several genes. As opposed to the traditional *P* value thresholds, the user balances the trade-off between false positives and the number of genes when deciding upon an acceptable *q* value threshold (25, 26). Calling the top 16 genes significant has the lowest false discovery rate (6.25%, or 1 gene called in error) in this experiment. Calling the top 21 genes significant induces a false discovery rate of 19%, or 4 genes called in error.

reveals (Table 1) that proteases (and in particular, mast-cell-derived proteases) are significantly changing their expression during the development of vascular obliteration. Statistical significance of these findings is compounded by experimental confirmation of the array-derived data, as shown in Fig. 5.

Mast cells are specialized immune effector cells that synthesize and store in their granules large amounts of serine proteases, which are classified as chymases (having chymotrypsin-like substrate specificity) or trypases (with trypsin-like substrate specificity) (13). Infiltration with mast cells is present in plexogenic pulmonary arteriopathy and in experimental models of pulmonary hypertension (10). In a case series of human pulmonary hypertension, chymase activity was detected

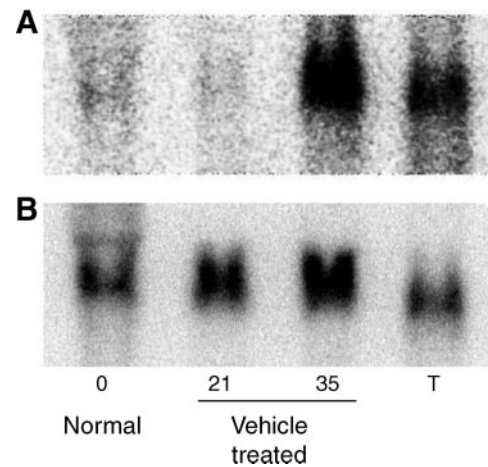


Fig. 5. Northern hybridization of mast cell protease-1 mRNA. A: Northern hybridization confirms the increase in mRNA levels of mast cell protease-1 at day 35 in vehicle-treated animals (35) and the partial attenuation of expression in triptolide-treated animals ("T") compared with normal animals ("0") and vehicle-treated diseased rats at day 21 ("21"). B: GAPDH mRNA levels from the same samples served as controls.

in vascular lesions with intimal fibrosis, suggesting the involvement of chymase-positive mast cells in vascular remodeling (15). Chymase and trypase are potent angiogenic signals in a variety of experimental models (4, 16).

We observed a 6.2-fold increase in expression between normal and diseased lungs (V35) of plasminogen activator inhibitor-1 (PAI-1). Our findings are concordant with other published data, such as the four- to fivefold increase of PAI-1 mRNA levels (as well as a corresponding increase of PAI-1 secretion) by normal pulmonary artery SMCs subjected to serial in vitro passages (2). Elevated plasma levels of PAI-1 [as well as tissue plasminogen activator (t-PA)] were found in a study of 10 patients with PPH compared with healthy controls (14).

Normal ECs do not produce significant amounts of PAI-1 in vivo, whereas in vitro they produce large amounts of PAI-1 (3). This discrepancy is explained by the absence in vitro of SMC-derived suppressive factor(s) (3). SMC proliferation is associated with upregulation of PAI-1 synthesis by both SMCs and ECs, as well as decreased t-PA production (2).

The balance between plasminogen activators and PAI-1 contributes to regulating cell migration within the extracellular

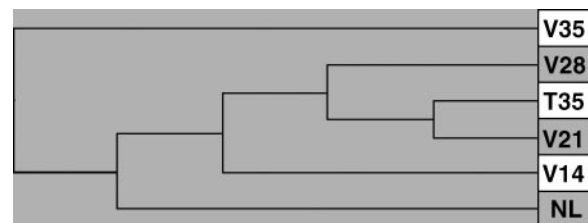


Fig. 6. Hierarchical clustering of experimental time points. Hierarchical clustering of global gene expression was performed, and the experimental time points are represented on a dendrogram. The fewer the nodes separating any pair of two time points, the more similar the global expressions of the time points are. Shorter branches are suggestive of more similarity compared with longer branches. The fully developed disease state (V35) has the most dissimilar global gene expression pattern, whereas treatment with triptolide (T35) restores global gene expression pattern to a state intermediate between days 21 and 28 in vehicle-treated animals (V21 and V28).

matrix (12). As a result of vascular injury (such as disruption of endothelial monolayer and basal membrane), serum thrombin comes in contact with SMC and not only acts as a mitogen on SMCs but also causes a fourfold increase in specific PAI-1 mRNA (as well as an increase in t-PA mRNA) and PAI-1 antigen levels in the extracellular matrix surrounding thrombin-exposed SMCs (31).

We found other proteases among the genes with significantly elevated expression during the development of pulmonary hypertension. For example, gelatinase A (matrix metalloproteinase-2), which degrades basement membrane components and promotes cell proliferation and migration, registers a fourfold increase at *day 35* compared with normal. The gelatinase activity correlates with the pulmonary hypertension severity in a monocrotaline model (9). Matrix metalloproteinase (MMP) expression and activity are increased in a rat model of chronic hypoxia-induced pulmonary hypertension (30).

Several cathepsins also increased their expression during the development of the disease.

Cathepsin K is a protease with potent fibrinolytic activity that may play an important role in extracellular matrix degradation. It is also closely involved in osteoclastic bone resorption and may participate partially in disorders of bone remodeling. Our results showing that mast cell chymases, MMPs, gelatinases, cathepsins, and PAI are increased during progression of pulmonary hypertension extend the observations that experimental pulmonary hypertension involves extensive remodeling of extracellular matrix (5).

Macrophage inflammatory protein-1 α (MIP-1 α) is a heparin-binding monokine with inflammatory properties that has chemotactic activity for monocytes, neutrophils, eosinophils, basophils, and lymphocytes. It is required for lung TNF- α production, neutrophil recruitment, and subsequent lung injury and may function as an autocrine mediator for the macrophage production of TNF- α , which in turn upregulates vascular adhesion molecules required for neutrophil influx.

IL-18 (IFN- γ inducing factor), a novel proinflammatory cytokine, involved in regulating inflammatory angiogenesis (21), is the only cytokine on the array (which also includes IL-1, IL-2, IL-6) to show a statistically significant variability in gene expression during the progression of this disease model.

Genes with an acute-phase expression pattern. A cluster of eight genes showed a transient increase in expression early after the two-step injury. This cluster included ErbB4, an epidermal growth factor (EGF) receptor present on human umbilical vein endothelial cells (HUVECS), ephrin receptors, and CNP, all of which may play a role in vascular remodeling. ErbB4 will induce EC proliferation and in vivo and in vitro angiogenesis (24). β -Cellulin, a member of the EGF family, is a potent mitogen for rat vascular SMCs (27) and induces angiogenesis through erbB4 (11).

Ephrin receptors play a crucial role in vascular development during embryogenesis, and the blockade of the EphA3 receptor inhibited tumoral angiogenesis and in vivo tumor growth (1). Ephrin B receptors also play well-established roles in angiogenesis (19), but their role in the adult is currently being defined. The role of ephrins 5 and 7 (the two members of the family that show up in this cluster) in vascular remodeling remains to be defined.

CNP is produced by ECs with local vasorelaxing and growth inhibitory effects. CNP decreases the EGF-induced EC prolif-

eration and capillary tube formation by human microvascular ECs (22).

Hierarchical clustering of experiments. The global gene expression at a time point may be construed as a "transcriptional fingerprint" that uniquely characterizes the given state. Hierarchical clustering of the experiments gives insight into how similar or dissimilar the global expressions are between experimental time points. Thus vehicle-treated animals at *day 35* (V35, when the disease is the most severe) stand out on an isolated branch of the dendrogram (Fig. 6), whereas triptolide-treated animals at *day 35* (T35) have an intermediate expression between the global expressions of V21 and V28. This shows an interesting correlation with the hemodynamics, which also show that the RVSP has been attenuated to a value intermediate between V21 and V28.

Our large-scale search of gene expression that parallels the pathophysiological evolution of experimental hypertensive pulmonary vascular disease (HPVD) resulted in identifying genes with expression changes that precede the development of pathology. Going further than the exploratory data analysis, we have confirmed the statistical significance of our findings using rigorous statistical methods. Finally, we have used classic biological validation of some of our findings. Although important differences exist between the proteases (specifically mast-cell-derived chymases and tryptases) of different species, the interface between thrombosis, inflammation, and dysregulated cell proliferation is clinically very relevant for the human disease PPH. Carefully conducted large-scale gene profiling studies with analysis of statistical significance and biologic correlation are likely to help us further understand the complex pulmonary vascular response to injury.

GRANTS

This work was supported by a gift from the Donald E. and Delia B. Baxter Foundation and by National Institutes of Health Grants AI-39624 and HL-62588 (to P. N. Kao).

REFERENCES

1. Brantley DM, Cheng N, Thompson EJ, Lin Q, Brekken RA, Thorpe PE, Muraoka RS, Cerretti DP, Pozzi A, Jackson D, Lin C, and Chen J. Soluble Eph A receptors inhibit tumor angiogenesis and progression in vivo. *Oncogene* 21: 7011–7026, 2002.
2. Christ G, Hufnagl P, Kaun C, Mundigler G, Laufer G, Huber K, Wojta J, and Binder BR. Antifibrinolytic properties of the vascular wall. Dependence on the history of smooth muscle cell doublings in vitro and in vivo. *Arterioscler Thromb Vasc Biol* 17: 723–730, 1997.
3. Christ G, Seiffert D, Hufnagl P, Gessl A, Wojta J, and Binder BR. Type 1 plasminogen activator inhibitor synthesis of endothelial cells is downregulated by smooth muscle cells. *Blood* 81: 1277–1283, 1993.
4. Coussens LM, Raymond WW, Bergers G, Laig-Webster M, Behrendt-sen O, Werb Z, Caughey GH, and Hanahan D. Inflammatory mast cells up-regulate angiogenesis during squamous epithelial carcinogenesis. *Genes Dev* 13: 1382–1397, 1999.
5. Cowan KN, Heilbut A, Humpl T, Lam C, Ito S, and Rabinovitch M. Complete reversal of fatal pulmonary hypertension in rats by a serine elastase inhibitor. *Nat Med* 6: 698–702, 2000.
6. Dysvik B and Jonassen I. J-Express: exploring gene expression data using Java. *Bioinformatics* 17: 369–370, 2001.
7. Faul JL, Nishimura T, Berry GJ, Benson GV, Pearl RG, and Kao PN. Triptolide attenuates pulmonary arterial hypertension and neointimal formation in rats. *Am J Respir Crit Care Med* 162: 2252–2258, 2000.
8. Fishman AP. Etiology and pathogenesis of primary pulmonary hypertension: a perspective. *Chest* 114: 242S–247S, 1998.
9. Frisdal E, Gest V, Vieillard-Baron A, Levame M, Lepetit H, Eddahibi S, Lafuma C, Harf A, Adnot S, and Dortho MP. Gelatinase expression in pulmonary arteries during experimental pulmonary hypertension. *Eur Respir J* 18: 838–845, 2001.

10. **Heath D and Yacoub M.** Lung mast cells in plexogenic pulmonary arteriopathy. *J Clin Pathol* 44: 1003–1006, 1991.
11. **Kim HS, Shin HS, Kwak HJ, Cho CH, Lee CO, and Koh GY.** Beta-cellululose induces angiogenesis through activation of mitogen-activated protein kinase and phosphatidylinositol 3'-kinase in endothelial cell. *FASEB J* 17: 318–320, 2003.
12. **Lang IM, Moser KM, and Schleef RR.** Elevated expression of urokinase-like plasminogen activator and plasminogen activator inhibitor type 1 during the vascular remodeling associated with pulmonary thromboembolism. *Arterioscler Thromb Vasc Biol* 18: 808–815, 1998.
13. **Lutzelschwab C, Pejler G, Aveskogh M, and Hellman L.** Secretory granule proteases in rat mast cells. Cloning of 10 different serine proteases and a carboxypeptidase A from various rat mast cell populations. *J Exp Med* 185: 13–29, 1997.
14. **Martin I, Humbert M, Marfaing-Koka A, Capron F, Wolf M, Meyer D, Simonneau G, and Angles-Cano E.** Plasminogen activation by blood monocytes and alveolar macrophages in primary pulmonary hypertension. *Blood Coagul Fibrinolysis* 13: 417–422, 2002.
15. **Mitani Y, Ueda M, Maruyama K, Shimpo H, Kojima A, Matsumura M, Aoki K, and Sakurai M.** Mast cell chymase in pulmonary hypertension. *Thorax* 54: 88–90, 1999.
16. **Muramatsu M, Katada J, Hayashi I, and Majima M.** Chymase as a proangiogenic factor. A possible involvement of chymase-angiotensin-dependent pathway in the hamster sponge angiogenesis model. *J Biol Chem* 275: 5545–5552, 2000.
17. **Nishimura T, Faul JL, Berry GJ, Vaszar LT, Qiu D, Pearl RG, and Kao PN.** Simvastatin attenuates smooth muscle neointimal proliferation and pulmonary hypertension in rats. *Am J Respir Crit Care Med* 166: 1403–1408, 2002.
18. **Nishimura T, Vaszar LT, Faul JL, Zhao G, Berry GJ, Shi L, Qiu D, Benson G, Pearl RG, and Kao PN.** Simvastatin rescues rats from fatal pulmonary hypertension by inducing apoptosis of neointimal smooth muscle cells. *Circulation* 108: 1640–1645, 2003.
19. **Oike Y, Ito Y, Hamada K, Zhang XQ, Miyata K, Arai F, Inada T, Araki K, Nakagata N, Takeya M, Kisanuki YY, Yanagisawa M, Gale NW, and Suda T.** Regulation of vasculogenesis and angiogenesis by EphB/ephrin-B2 signaling between endothelial cells and surrounding mesenchymal cells. *Blood* 100: 1326–1333, 2002.
20. **Okada K, Tanaka Y, Bernstein M, Zhang W, Patterson GA, and Botney MD.** Pulmonary hemodynamics modify the rat pulmonary artery response to injury. A neointimal model of pulmonary hypertension. *Am J Pathol* 151: 1019–1025, 1997.
21. **Park CC, Morel JC, Amin MA, Connors MA, Harlow LA, and Koch AE.** Evidence of IL-18 as a novel angiogenic mediator. *J Immunol* 167: 1644–1653, 2001.
22. **Pedram A, Razandi M, and Levin ER.** Natriuretic peptides suppress vascular endothelial cell growth factor signaling to angiogenesis. *Endocrinology* 142: 1578–1586, 2001.
23. **Rubin LJ.** Primary pulmonary hypertension. *N Engl J Med* 336: 111–117, 1997.
24. **Russell KS, Stern DF, Polverini PJ, and Bender JR.** Neuregulin activation of ErbB receptors in vascular endothelium leads to angiogenesis. *Am J Physiol Heart Circ Physiol* 277: H2205–H2211, 1999.
25. **Storey JD.** A direct approach to false discovery rates. *J R Stat Soc* 64: 479–498, 2002.
26. **Storey JD and Tibshirani R.** Statistical significance for genomewide studies. *Proc Natl Acad Sci USA* 100: 9440–9445, 2003.
27. **Tamura R, Miyagawa J, Nishida M, Kihara S, Sasada R, Igarashi K, Nakata A, Yamamori K, Kameda-Takemura K, Yamashita S, and Matsuzawa Y.** Immunohistochemical localization of beta-cellululose, a member of epidermal growth factor family, in atherosclerotic plaques of human aorta. *Atherosclerosis* 155: 413–423, 2001.
28. **Tanaka Y, Bernstein ML, Mecham RP, Patterson GA, Cooper JD, and Botney MD.** Site-specific responses to monocrotaline-induced vascular injury: evidence for two distinct mechanisms of remodeling. *Am J Respir Cell Mol Biol* 15: 390–397, 1996.
29. **Tusher VG, Tibshirani R, and Chu G.** Significance analysis of microarrays applied to the ionizing radiation response. *Proc Natl Acad Sci USA* 98: 5116–5121, 2001.
30. **Vieillard-Baron A, Frisdal E, Eddahibi S, Deprez I, Baker AH, Newby AC, Berger P, Levame M, Raffestin B, Adnot S, and d'Ortho MP.** Inhibition of matrix metalloproteinases by lung TIMP-1 gene transfer or doxycycline aggravates pulmonary hypertension in rats. *Circ Res* 87: 418–425, 2000.
31. **Wojta J, Gallicchio M, Zoellner H, Hufnagl P, Last K, Filonzi EL, Binder BR, Hamilton JA, and McGrath K.** Thrombin stimulates expression of tissue-type plasminogen activator and plasminogen activator inhibitor type 1 in cultured human vascular smooth muscle cells. *Thromb Haemostasis* 70: 469–474, 1993.
32. **Zhao G, Vaszar LT, Qiu D, Shi L, and Kao PN.** Anti-inflammatory effects of triptolide in human bronchial epithelial cells. *Am J Physiol Lung Cell Mol Physiol* 279: L958–L966, 2000.